GeoStruct Innovations
https://www.acadlore.com/journals/GSI

Failure Criteria for Subway Tunnels Based on the Load-Unload Response Ratio Theory

Yichao Chen, Honglin Cao, Changchao Tian*, Jianbin Sun, Wenhua Ji

Shandong Transportation Institute, 250031 Jinan, China

* Correspondence: Changchao Tian (416851668@qq.com)

Received: 03-28-2024 **Revised:** 05-18-2024 **Accepted:** 06-03-2024

Citation: Y. C. Chen, H. L. Cao, C. C. Tian, J. B. Sun, and W. H. Ji, "Failure criteria for subway tunnels based on the load-unload response ratio theorye," *GeoStruct. Innov.*, vol. 2, no. 2, pp. 68–76, 2024. https://doi.org/10.56578/gsi020202.

Abstract: This study employs a combination of geological investigation, numerical simulation, and theoretical analysis to evaluate the applicability of the load-unload response ratio (LURR) theory in urban tunnels. The results indicate that using the sudden increase in the LURR at critical points or the equivalent plastic strain penetration between the tunnel and the ground surface as failure criteria for subway tunnels is feasible. Under critical instability loads, the equivalent plastic strain zones in the surrounding rock penetrate to the surface during the construction phase, leading to severe deformation of the tunnel chamber group and loss of load-bearing capacity in the surrounding rock. During the operation phase, the tunnel lining plays a primary load-bearing role. Under instability loads, a butterfly-shaped failure zone appears in the surrounding rock. These findings can be utilized for the quantitative evaluation of the overall safety margin of urban subway tunnels.

Keywords: Subway tunnel; Load-unload response ratio; Equivalent plastic strain; Failure criteria

1 Introduction

The construction of urban subway tunnels is often undertaken in complex environments and geological conditions, where surface collapses frequently occur during the construction process [1, 2], posing significant hazards and severely disrupting the normal functioning of urban areas. Due to the shallow depth of subway tunnels, which are often located beneath municipal roads or buildings, frequent load disturbances occur. The essence of surface subsidence is the instability and failure of the surrounding rock caused by excavation. Therefore, analyzing the failure modes of the surrounding rock and establishing failure criteria through numerical simulation studies is crucial for predicting surface collapse incidents and developing preventive measures.

In recent years, the determination of tunnel failure has been one of the key technical challenges in engineering construction due to the complexity of the mechanical properties and deformation mechanisms of rock masses. To quantitatively assess the stability of tunnel projects, Zhang et al. [3] were among the first to propose the concept of a safety factor for the surrounding rock based on the strength reduction method (SRM), using the abrupt displacement of the surrounding rock as the criterion. The SRM was applied to solve the potential failure surface of the tunnel, revealing the evolution characteristics of elastic energy and dissipative energy during rock loading failure [4]. Shiau et al. [5] used the shear SRM within a two-dimensional finite element limit analysis program to obtain strict upper and lower bounds of safety factors for different depth ratios and centre-to-centre distance ratios between tunnels. The SRM was combined with numerical simulation to achieve the gradual fracture process of deep rock masses, revealing macroscopic failure modes and solving for safety factors [6, 7]. Sun et al. [8] utilized a combination of inverse analysis and the SRM to quantify tunnel stability during construction. In addition, the application of the limit equilibrium method and the SRM in geotechnical engineering was compared, proposing a new approach for evaluating the stability of tunnel faces [9, 10].

According to rock mechanics theory, the mechanical parameters of rock masses gradually weaken over time due to the presence of in-situ stress environments. Consequently, the SRM is more suitable for deeply buried tunnels and less applicable to shallow tunnels with lower in-situ stress. The LURR method, based on surface load and unload, better aligns with the working conditions of urban subway tunnels. Discrete element was utilized to simulate the mechanical behaviour of inclined jointed rock layers during tunnel excavation, employing indicators such as

vertical, horizontal, and total displacements to comprehensively assess the stability of jointed rock mass tunnels during excavation [11, 12]. Zhang et al. [13] applied the LURR method to detect the nonlinear deformation process of strain-stress curves, assessing the degree of rock damage and instability fracture. Tan et al. [14] introduced the LURR theory into the stability calculation of shallow tunnels, using the sudden increase in the response ratio growth rate at critical deformation points around the tunnel as a criterion for tunnel instability, and proposed a method for determining tunnel instability based on the LURR.

In recent years, both domestic and international experts have made some progress in understanding the failure mechanisms and establishing failure criteria for surrounding rock in tunnels. However, most of the research has focused on deeply buried or mountainous tunnels, with relatively few studies addressing the deformation and failure of surrounding rock in urban subway tunnels, due to their unique characteristics. The rules obtained for mountainous tunnels are difficult to apply to urban subway tunnels. Therefore, this study, based on a subway tunnel project, employs a combination of geological investigation, numerical simulation, and theoretical analysis to explore the feasibility of using the LURR method for the quantitative evaluation of the stability of surrounding rock in subway tunnels. The findings of this study are expected to provide a reference for the design of support structures in urban subway tunnels.

2 LURR Theory

The LURR theory [14] is primarily based on the concept that nonlinear systems can exhibit significant responses under minimal load. The ratio Y of the load response rate to the unload response rate is used to quantitatively describe the extent to which a system approaches an unstable state. For a nonlinear system, the relationship between the load P and the response parameter R is illustrated in Figure 1. The response rate X_i for the i-th cycle step is defined as follows [14]:

$$X_i = \frac{\Delta R_i}{\Delta P_i} \tag{1}$$

where, ΔP_i is the increment of the load P, and ΔR_i is the corresponding response increment under the load increment ΔP_i. The LURR Y_i is defined as follows:

$$Y_i = \frac{X_i^+}{X_{i-1}^-} \tag{2}$$

where, X_i^+ is the load response rate for the i-th cycle step, and X_{i-1}^- is the unload response rate for the (i-1)-th cycle step.

According to the characteristics of the incremental displacement response ratio parameter, when $Y_i < 1$, the surrounding rock is in the elastic stage, and the tunnel chamber group remains in a stable state. When $Y_i > 1$, the surrounding rock enters the elastoplastic stage, and the tunnel chamber group tends toward an unstable state. When $Y_i \to \infty$, the LURR increases monotonically, leading to instability and gradual failure of the tunnel chamber group.

In this study, a vertical stress-total displacement load-deformation response ratio evaluation model was established for the tunnel crown. The model is defined as follows: the deformation of characteristic key points in the tunnel during excavation was considered as the load-unload response parameter. The change in vertical stress at the tunnel crown, ΔP_i, was regarded as the load increment, and the corresponding change in total displacement, ΔP_i, was taken as the response parameter. This model forms the basis for the static load-deformation response ratio evaluation model for the tunnel. It is expressed as follows:

$$Y_i = \frac{X_i^+}{X_{i-1}^-} = \frac{\Delta R_i^+ / \Delta P_i^+}{\Delta R_{i-1}^- / \Delta P_{i-1}^-} = \frac{\Delta S_i^+ / \Delta \sigma_i^+}{\Delta S_{i-1}^- / \Delta \sigma_{i-1}^-} \tag{3}$$

where, ΔS_i^+ and ΔS_{i-1} are the deformation response quantities at the i-th and (i-1)-th steps, respectively, and $\Delta \sigma_i^+$ and $\Delta \sigma_{i-1}$ are the corresponding vertical stress response quantities at the i-th and (i-1)-th steps, respectively; and i=1,2,.....,n.

To avoid dynamic effects, load and unload were applied to the model boundaries based on the initial stress state of the surrounding rock. This approach prevented variations in load and unload conditions caused by different stress states of the surrounding rock, and adhered to the core principles of the LURR study. The load and unload process in the model was implemented by incrementally applying surface loads in cycles. Surface uniform loads were gradually applied in steps, with a load increment of W=20 KPa for each cycle, based on a unit soil layer thickness of 1 meter. A disturbance cycle was introduced during this process, with each cycle consisting of three calculation steps: two loading steps followed by one unloading step. The specific calculation for the applied loads is given by Eq. (4), and a schematic of the load application is illustrated in Figure 1.

$$P = A\left\{ \text{quotient}\,(t,3) + \sin\left[\frac{\pi}{2}(\text{mod}(t,3)-1)\right]\right\} \tag{4}$$

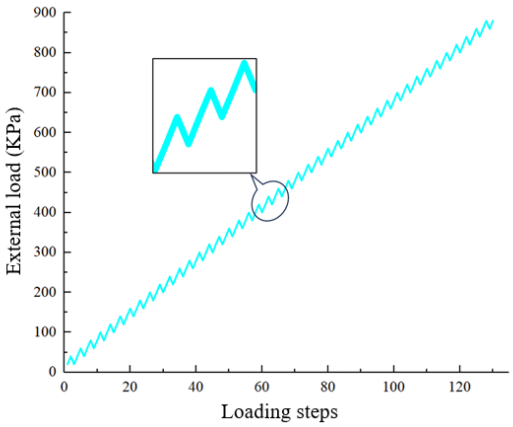

Figure 1. Schematic of the load-unload process

3 Project Background and Numerical Model

The subway tunnel under study has a clear width of 11 meters and a clear height of 5 meters, with a horseshoe-shaped cross-section. The surrounding rock is composed of highly weathered granite, characterized by well-developed joints, and classified as Grade V rock mass. The overall boundary of the surrounding rock model is set at a horizontal distance of 40 meters from the tunnel boundary on both sides, a vertical distance of 40 meters below the tunnel, and a distance of 15 meters from the surface for the shallowly buried tunnel. The geotechnical layer is considered an isotropic, ideal elastic-plastic material with a dominant structural plane (dip angle 72°, dip direction 58°) following the Mohr-Coulomb (M-C) criterion. To ensure stable loading and computational efficiency, the model thickness is set as two excavation advances, totaling 4 meters. Horizontal constraints were applied to the left and right boundaries of the model, while fixed constraints were applied to the bottom boundary. Calculations were performed for both the construction and operation phases, using equivalent plastic strain and the LURR as the computational parameters to determine the instability loads and failure surfaces under different conditions. The mechanical parameters of the rock mass and lining are provided in Table 1. The mechanical parameters of the structural plane are listed in Table 2. The computational model and loading arrangement are illustrated in Figure 2 and Figure 3.

Table 1. Physical and mechanical parameters of the rock mass

Rock Mass Grade	Density $(\mathbf{kg/m^3})$	Bulk Modulus $(\mathbf{Pa})$	Cohesion $(\mathbf{Pa})$	Internal Friction Angle $(°)$	Shear Strength $(\mathbf{Pa})$
V	2000	1.11×10^9	0.50×10^5	25	3.70×10^8
Lining	2600	1.83×10^{10}	3.00×10^6	50	8.46×10^9

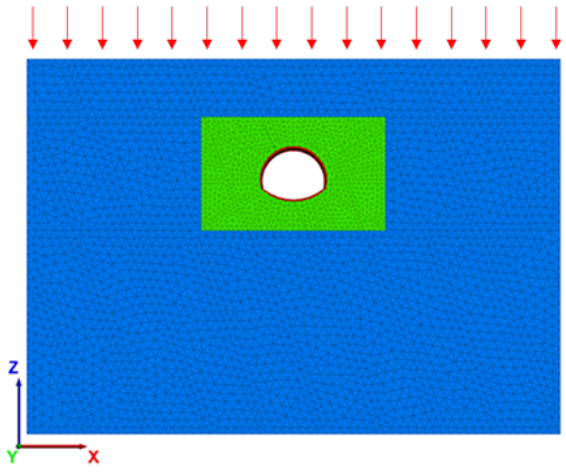

Figure 2. Schematic diagram of the computational model and loading arrangement

Table 2. Physical and mechanical parameters of the structural plane

Normal Stiffness (Pa)	Shear Stiffness (Pa)	Cohesion (Pa)	Internal Friction Angle (°)
0.80×10^{10}	5.00×10^{9}	3.41×10^{5}	34.8

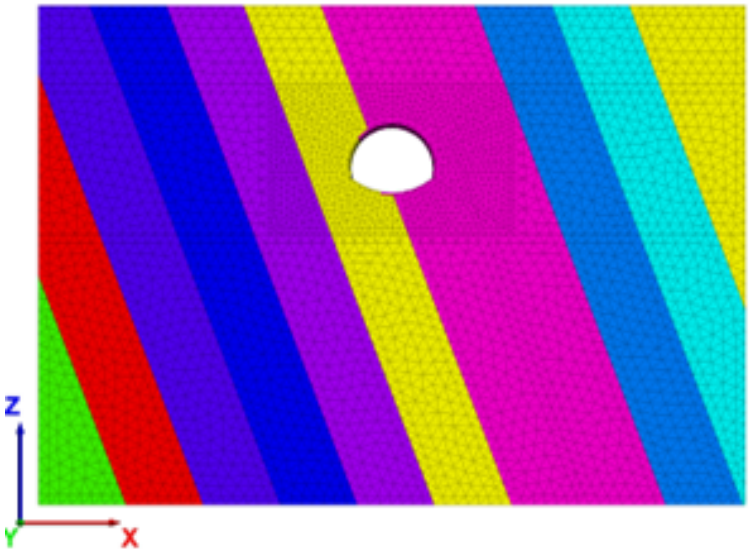

Figure 3. Schematic diagram of the structural plane arrangement

Based on the mechanical characteristics of tunnel excavation, the deformation of key characteristic points in the tunnel was determined as the load-unload response parameters. These points include the tunnel crown (Point 1), the inverted arch waist (Point 2), the arch waist (Point 3), the arch foot (Point 4), and two points at the tunnel bottom (Points 5 and 6), as illustrated in Figure 4.

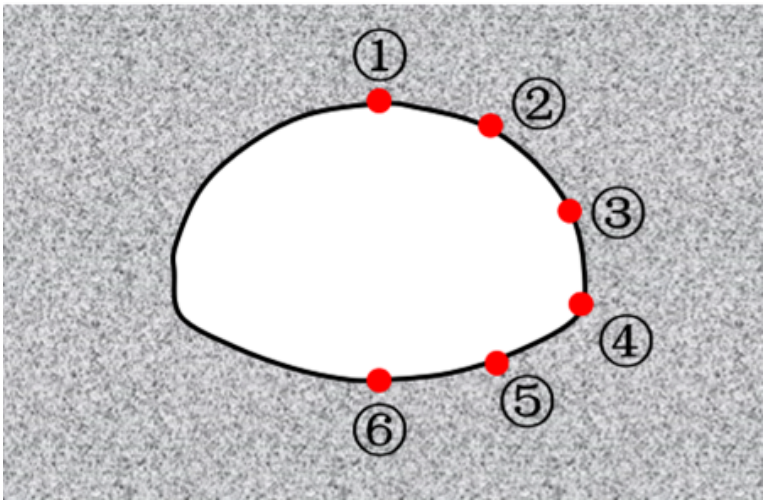

Figure 4. Locations of the monitoring points

4 LURR Results and Stability Analysis of the Tunnel under Surface Loading

During the construction process, the tunnel primarily bears the load resulting from the release of surrounding rock stress due to the excavation of the geotechnical body. Given the differing stress mechanisms between the construction phase (excavation without support) and the operational phase (excavation with support), this section separately examines the stability of the surrounding rock during these two phases.

After completing the excavation, the load was applied to the top of the model according to Eq. (4), and the LURR for each unit was calculated using FISH programming.

The results of the LURR analysis for the deformation of key tunnel points under different conditions are presented in Figure 5 and Figure 6. The equivalent plastic strain zones of the surrounding rock and lining are shown in Figure 7, Figure 8, and Figure 9.

As shown in Figure 5, the LURR for the deformation of key tunnel points during the construction phase can be broadly divided into two groups: monitoring points 2, 3, and 4, and monitoring points 1, 5, and 6. Without support, the initial LURR of the surrounding rock is greater than 1, indicating that the rock mass has already entered a plastic state before loading during the construction phase [14]. As the load and unload continue, the LURR gradually increases, with a significant surge in the response ratio curves at monitoring points 2, 3, and 4 occurring at a load of 240 KPa. This indicates that the surrounding rock on both sides of the tunnel has experienced failure, particularly on the side closer to the structural plane, where the equivalent plastic strain value is nearly double that of the corresponding position on the opposite side. This suggests that the structural plane has a substantial impact on the tunnel excavation. The response ratio curves at monitoring points 1, 5, and 6 exhibit a similar pattern, although with a noticeable delay compared to points 2, 3, and 4. A sharp increase in the response ratio occurs at a load of 360 KPa, with the response ratio at the arch waist showing a greater value and increasing earlier than at the tunnel bottom and crown. This indicates that the arch waist of this subway tunnel is more vulnerable compared to the tunnel bottom and crown.

As shown in Figure 6, the LURR curve during the operational phase can be roughly divided into three stages based on load variation: the stages of stable growth, fluctuating growth, and instability growth. In the stable growth stage, the slope of the LURR curve remains constant, indicating a nearly linear increase with the applied load. In the fluctuating growth stage, the slope of the LURR curve alternates between positive and negative, resulting in an overall fluctuating increase. In the instability growth stage, the slope of the LURR curve experiences a sudden increase, and the LURR shows a trend of non-convergence.

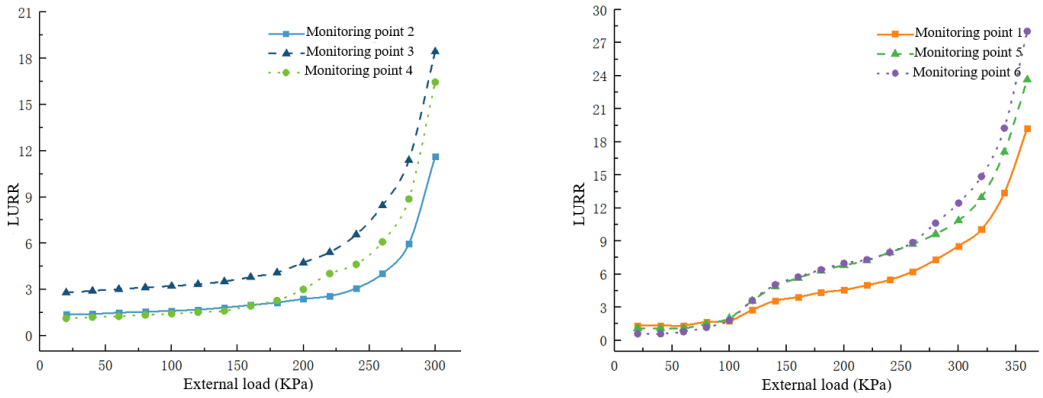

(a) (b)

Figure 5. Comparison of LURR results for deformation of key tunnel points during the construction phase

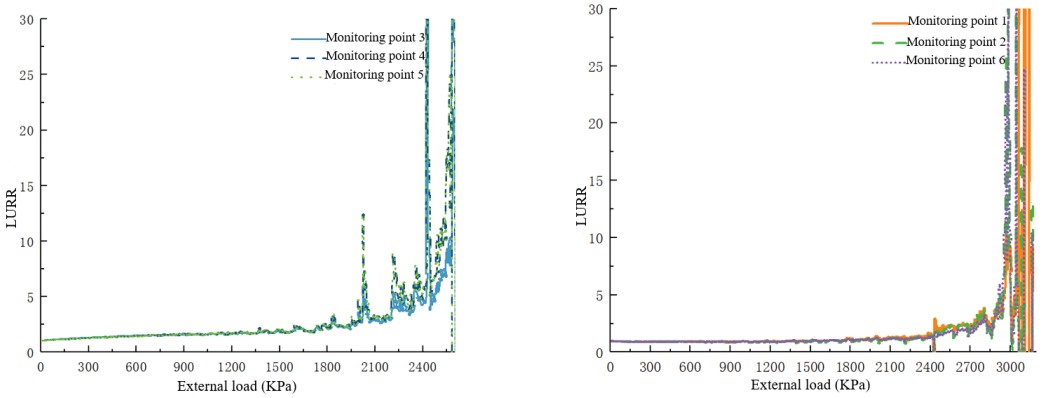

(a) (b)

Figure 6. Comparison of LURR results for deformation of key tunnel points during the operational phase

As depicted in Figure 6, unlike during the construction phase, the LURR for the deformation of key tunnel points during the operational phase can be grouped into two categories: monitoring points 3, 4, and 5, and monitoring points 1, 2, and 6. This distinction suggests that the stress and deformation mechanisms of the supported and unsupported surrounding rock are different. When the surface load reaches 2020 KPa, a sudden increase in the LURR is observed at monitoring points 3, 4, and 5. Similarly, a sudden increase occurs at monitoring points 1, 2, and 6 when the surface load reaches 2960 KPa. The load at which the sudden increase occurs after the support is applied is nearly ten times that of the unsupported case, indicating the significant effect of the support. The increase in the LURR is more pronounced under support, with only the fluctuating growth of the response ratio curve as a precursor, suggesting that once structural failure occurs in the tunnel under support, the impact on the surrounding rock is more severe. Therefore, in the operational monitoring process, any detection of fluctuating growth in the curve should prompt immediate reinforcement measures.

The cloud map of equivalent plastic strain under surface loading during the construction phase is shown in Figure 7. As the load increases, surface settlement gradually intensifies, and plastic strain zones begin to appear on both sides of the tunnel, gradually extending to the surface. This corresponds to the first sudden increase in the LURR curve as the load reaches 240 KPa. At this point, the equivalent plastic strain zones on both sides of the tunnel exhibit significant values, with the plastic strain zone on the right side, closer to the structural plane, connecting to the structural plane. The area of this zone is more than three times larger than that of the corresponding zone on the left side. The plastic strain zones around the tunnel have already penetrated to the surface, resulting in a loss of load-bearing capacity.

The cloud maps of equivalent plastic strain under load-unload conditions during the operational phase are shown in Figure 8 and Figure 9. As the load increases (0 1060 KPa), the plastic strain zones are concentrated in the lining base and both sides of the tunnel, with the depth of the plastic strain zones in the surrounding rock being relatively shallow. As the load continues to increase, the plastic strain zones in the surrounding rock begin to extend significantly towards the bottom and both sides of the tunnel, forming a butterfly-shaped failure zone [15]. Coinciding with the first sudden increase in the LURR curve as the surface load reaches 2020 KPa, the equivalent plastic strain zones on both sides of the tunnel have already penetrated extensively to the surface. The plastic strain values at the lining base and both sides of the tunnel become substantial, indicating a loss of load-bearing capacity.

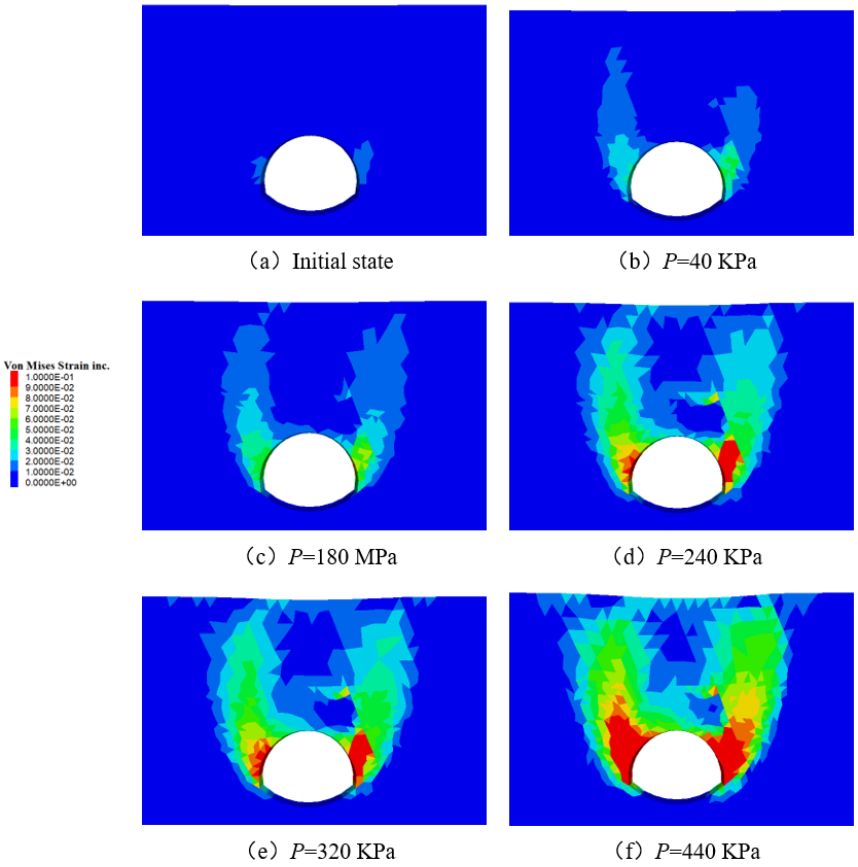

Figure 7. Changes in equivalent plastic strain of surrounding rock under load-unload conditions during the construction phase

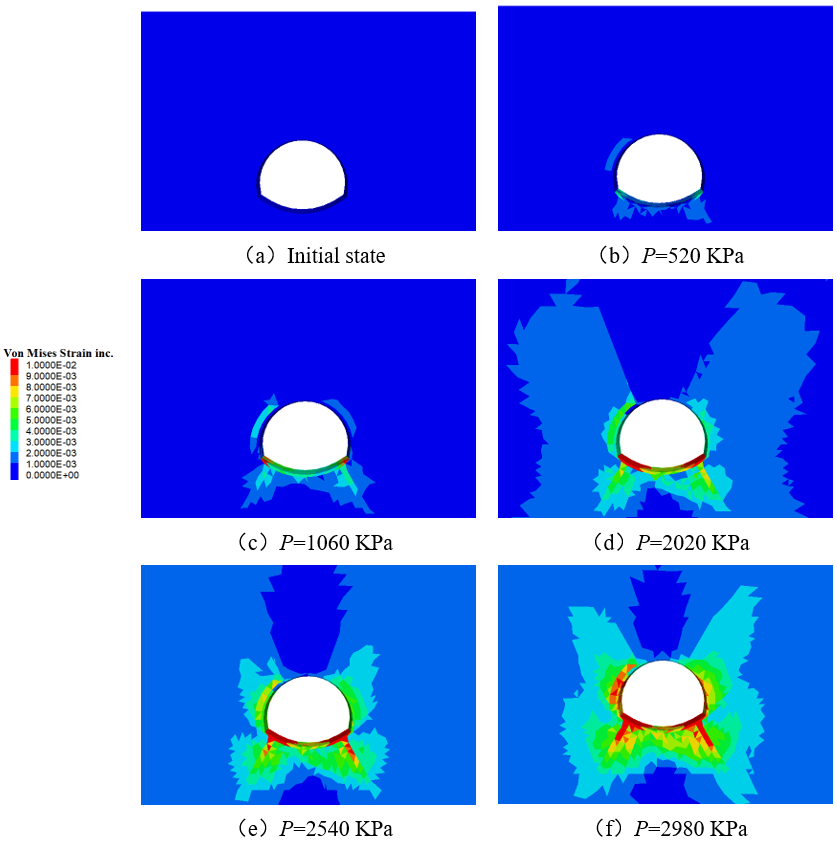

Figure 8. Changes in equivalent plastic strain of surrounding rock under load-unload conditions during the operational phase

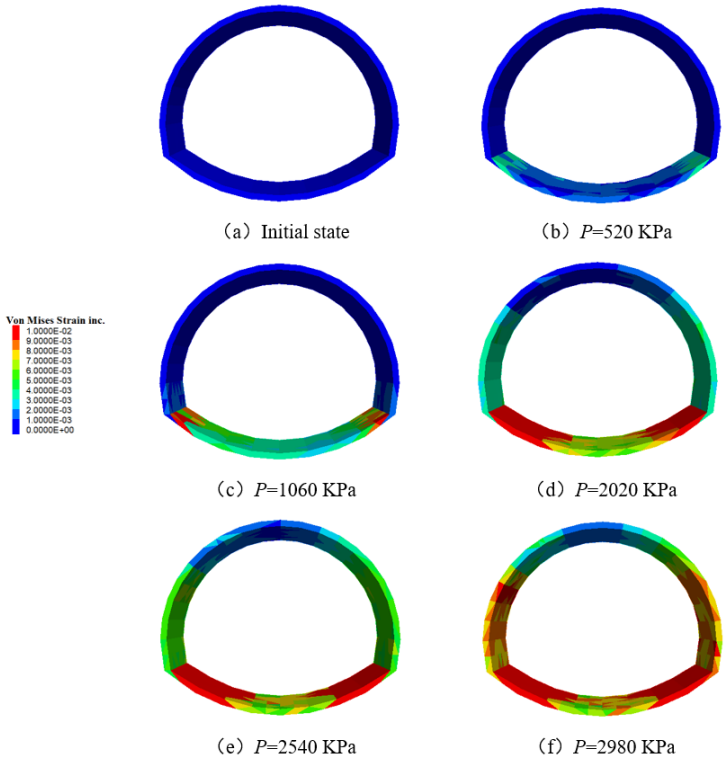

Figure 9. Changes in equivalent plastic strain of tunnel support under load-unload conditions during the operational phase

From the analysis of the LURR characteristics at key points and the changes in equivalent plastic strain zones with varying loads, when using the sudden increase in the LURR at key points as a criterion for the overall instability of the tunnel chamber group, the instability loads during the construction and operational phases were found to be 240 KPa and 2020 KPa, respectively. During the construction phase, the surrounding rock, when unsupported, readily enters a plastic state. With even a small increase in load, the equivalent plastic strain zone penetrates to the surface. At the instability load, the equivalent plastic strain zone has fully penetrated to the surface, resulting in severe tunnel deformation and a loss of load-bearing capacity in the surrounding rock. This indicates that timely support during the construction phase is crucial to prevent tunnel failure induced by surface loads.

5 Conclusion

Using FISH language programming, the LURR method was integrated into discrete element numerical simulation software to calculate two classic cases during the construction and operational phases of an urban subway tunnel. The main conclusions are as follows:

(a) It is feasible to quantitatively evaluate the overall safety margin of subway tunnels based on the LURR theory. In the calculation process, the sudden increase in the LURR at key points was adopted as a criterion for overall tunnel instability. The instability loads during the construction and operational phases are 240 KPa and 2020 KPa, respectively. When using the equivalent plastic strain penetration between the tunnel and the surface as the critical criterion for subway tunnel failure, the instability loads are nearly identical. In practice, when the equivalent plastic strain zones coalesce between tunnel chambers, the LURR also exhibits a sudden increase, and the calculation process tends to diverge, indicating a synchronous consistency between the two phenomena.

(b) The calculations for two typical cases during the construction and operational phases of a subway tunnel demonstrate that the surrounding rock during the construction phase, when unsupported, easily enters a plastic state, particularly on the side near the structural plane. With even a small increase in load, the equivalent plastic strain zone penetrates to the surface, resulting in severe tunnel deformation and loss of load-bearing capacity in the surrounding rock. During the operational phase, under critical instability loads, the plastic strain zone at the lining base becomes significant, and a butterfly-shaped failure zone appears in the surrounding rock. These findings provide a scientific basis for the excavation and support design of subway tunnels.

Data Availability

The data used to support the research findings are available from the corresponding author upon request..

Conflicts of Interest

The authors declare no conflict of interest.

References

[1] J. Wang, G. Lin, G. Xu, Y. Wei, S. Li, X. Tang, and C. He, "Face stability of EPB shield tunnels in multilayered ground with soft sand lying on hard rock considering dynamic excavation process: A DEM study," *Tunn. Undergr. Space Technol.*, vol. 120, p. 104268, 2022. https://doi.org/10.1016/j.tust.2021.104268

[2] S. Guo, B. Wang, P. Zhang, S. Wang, Z. Guo, and X. Hou, "Influence analysis and relationship evolution between construction parameters and ground settlements induced by shield tunneling under soil-rock mixed-face conditions," *Tunn. Undergr. Space Technol.*, vol. 134, p. 105020, 2023. https://doi.org/10.1016/j.tust.2023.105020

[3] L. Zhang, Y. Zheng, Z. Wang, and J. Wang, "Application of strength reduction finite element method to road tunnels," *Rock Soil Mech.*, vol. 2007, no. 1, pp. 97–101+106, 2007. https://doi.org/10.3969/j.issn.1000-7598.2007.01.018

[4] L. Zhang, W. Chao, Z. Liu, Y. Cong, and Z. Wang, "Crack propagation characteristics during progressive failure of circular tunnels and the early warning thereof based on multi-sensor data fusion," *Geomech. Geophys. Geo-Energy Geo-Resour.*, vol. 8, p. 172, 2022. https://doi.org/10.1007/s40948-022-00482-3

[5] J. Shiau and F. Al-Asadi, "Stability analysis of twin circular tunnels using shear strength reduction method," *Géotechnique Lett.*, vol. 10, no. 2, pp. 311–319, 2020. https://doi.org/10.1680/jgele.19.00003

[6] B. Chen, B. Gong, S. Wang, and C. Tang, "Research on zonal disintegration characteristics and failure mechanisms of deep tunnel in jointed rock mass with strength reduction method," *Mathematics*, vol. 10, no. 6, p. 922, 2022. https://doi.org/10.3390/math10060922

[7] J. Yang, W. Chen, D. Yang, and J. Yuan, "Numerical determination of strength and deformability of fractured rock mass by FEM modeling," *Comput. Geotech.*, vol. 64, pp. 20–31, 2015. https://doi.org/10.1016/j.compgeo.2014.10.011

[8] J. Sun, F. Wang, X. Wang, and X. Wu, "A quantitative evaluation method based on back analysis and the double-strength reduction optimization method for tunnel stability," *Adv. Civ. Eng.*, vol. 2021, no. 1, pp. 1–14, 2021. https://doi.org/10.1155/2021/8899685

[9] F. Huang, Z. Li, and T. Ling, "Upper bound solution of safety factor for shallow tunnels face using a nonlinear failure criterion and shear strength reduction technique," *Math. Probl. Eng.*, vol. 2016, no. 1, p. 4832097, 2016. https://doi.org/10.1155/2016/4832097

[10] F. Tschuchnigg, H. F. Schweiger, S. W. Sloan, A. V. Lyamin, and I. Raissakis, "Comparison of finite-element limit analysis and strength reduction techniques," *Geotechnique*, vol. 65, no. 4, pp. 249–257, 2015. https://doi.org/10.1680/geot.14.p.022

[11] S. He, Y. Li, and A. Aydin, "A comparative study of UDEC simulations of an unsupported rock tunnel," *Tunn. Undergr. Space Technol.*, vol. 72, pp. 242–249, 2018. https://doi.org/10.1016/j.tust.2017.11.031

[12] T. N. Do and J. Wu, "Simulation of the inclined jointed rock mass behaviors in a mountain tunnel excavation using DDA," *Comput. Geotech.*, vol. 117, p. 103249, 2020. https://doi.org/10.1016/j.compgeo.2019.103249

[13] S. Zhang, R. Yang, J. Tan, Y. Zhang, and J. Jiang, "The evolution characteristics of rock fracture instability under cyclic loading on the basis of the enhanced LURR," *Front. Earth Sci.*, vol. 2023, no. 10, p. 1069046, 2023. https://doi.org/10.3389/feart.2022.1069046

[14] X. Tan, F. Gao, and W. Xu, "Static instability criterion and safety factor of tunnels based on loading/unloading response ratio," *Chin. J. Geotech. Eng.*, vol. 44, no. 9, pp. 1644–1653, 2022. https://doi.org/10.11779/CJGE202209009

[15] C. Yuan, L. Cao, L. Fan, and J. Guo, "Theoretical analysis on distribution pattern of plastic zone in surrounding rock of high-gas-coal roadway," *Adv. Civ. Eng.*, vol. 2021, no. 1, p. 6684243, 2021. https://doi.org/10.1155/2021/6684243